The new INFN-CHNet neutron imaging facility

The new INFN-CHNet neutron imaging facility

Gelli, N.[1], Giuntini, L.[1,2], Cantini, F.[1,2,3], Sans-Planell, O.[4,5], Magalini M. [4,5], Manetti,M.[1], Sodi L. [1], Massi, M. [1], Castelli, L.[1], Czelusniak, C.[1], Taccetti, F.[1], Bella T.E.[6], Marcucci G.[7,8,9], Clemenza, M.[7,8], Di Martino D.[7,8], Morigi, M.[10,11],Bettuzzi, M.[10,11], Vigorelli, L.[4,5,12], Re, A.[4,5], Lo Giudice, A.[4,5], Alloni, D. [13,14], Prata, M.[13,14,*] ,Altieri, S.[13,15], Salvini,A.[13,14], and Grazzi F.[1,3]

1 INFN Sezione di Firenze, Italy
2 Dipartimento di Fisica e Astronomia, Università degli Studi di Firenze, Italy
3 Consiglio Nazionale delle Ricerche, Istituto di Fisica Applicata “Nello Carrara”, Sesto Fiorentino, Italy
4 INFN, Sezione di Torino, Torino, Italy
5 Dipartimento di Fisica, Università degli Studi di Torino, Italy
6 Independent researcher
7 INFN Sezione di Milano Bicocca, Milano, Italy
8 Dipartimento di Fisica “G. Occhialini”, Università di Milano Bicocca, Milano, Italy
9 ISIS Facility, UKRI-STFC, Rutherford Appleton Laboratory, Didcot, UK
10 INFN Sezione di Bologna, Italy
11 Dipartimento di Fisica ed Astronomia "Augusto Righi", Università di Bologna, Italy 12 Dipartimento di Elettronica e Telecomunicazioni, Politecnico di Torino, Italy
13 INFN Sezione di Pavia, Italy
14 Laboratorio Energia Nucleare Applicata (LENA), Pavia, Italy
15 Dipartimento di Fisica, Università di Pavia, Italy
*Now at European Commission, Joint Research Centre, Ispra (VA), Italy

Abstract: In this paper, NICHE (Neutron Imaging for Cultural HEritage), the new neutron imaging facility of the Italian National Institute of Nuclear Physics (INFN) is shortly presented. We report on the main features of the beamline, the specifications of the detection set-up, and the performances of the imaging system. NICHE is installed at the TRIGA reactor of LENA (Laboratorio Energia Nucleare Applicata) Pavia University laboratory (Italy). The imaging facility was designed during 2020, installed in the spring 2021, and has been in operation since May 2021. NICHE is the first Italian neutron imaging station open to national external users through the INFN-CHNet network application system. NICHE allows users to obtain neutron radiographies and tomographies, thus allowing for morphological characterisation of samples. First results to highlight the potential of the facility are reported. In particular, we show the first results about spatial resolution measurement and 3D reconstruction to provide morphological analysis capabilities.

KEYWORDS: neutron imaging; neutron tomography; thermal neutron, morphological analysis; cultural heritage application

Introduction

The Cultural Heritage Network INFN-CHNet is a research infrastructure, widespread all over Italy, of the Istituto Nazionale di Fisica Nucleare (INFN) dedicated to the development and the applications of analytical techniques to perform advanced diagnostic on materials and artefacts related to Cultural Heritage (CH) [1]. It is based on several research centres, both in Italy and abroad, where cutting-edge technologies are developed and optimised in order to address the needs of Cultural Heritage researchers, such as archaeologists, historians, art historians, restorers, and conservators, as regards diagnostic features [2].

Within CHNet, many complementary analytical techniques are available whose scientific output quality is continuously improved and upgraded. The use of different analysis and diagnostic technologies provides complementary information aiming at facilitating the application of the best practices for restoration/conservation. Analyses are also useful for characterising materials and manufacturing techniques, studying the provenance of the raw materials, and giving indications about material authenticity.

Until 2021, neutron imaging (NI) was not available within CHNet, notwithstanding its tailored features for nondestructively evaluating sample morphology. NI integrates/complements results from well-known and widelyused X-ray radiography and tomography.

NI is a well-established election technique in the study of various metal composite samples [3-11], as different metals cannot be penetrated or measured with a relevant contrast factor in X-ray imaging while they exhibit reasonable transparency and relevant contrast in neutron radiography. Analogously, organic materials containing hydrogen can be visualised using NI, although surrounded by metal, a result very hard to achieve using X-rays [4].

These are the main reasons that led to the conception and implementation of the INFN-CHNet NICHE facility, described in this paper. The new NI station, developed in the framework of the NICHE experiment, was installed at the thermal beam port channel B of the TRIGA reactor of Laboratorio Energia Nucleare Applicata (LENA), in Pavia (Italy).

NICHE: presentation and overview

In recent years, the efficiency of digital imaging systems as well as the light yield of scintillator-based neutron detectors improved in sensitivity, dynamic range and linearity thus it makes possible to perform imaging analysis even at weak neutron sources. This allows to exploit small neutron sources, such as low-power research reactors (e.g. the TRIGA type [12]) and accelerator driven sources [13] to perform good quality NI.

The quality of NI data depends on the beam properties, such as neutron flux, collimation, beam size, and background noise (environmental and detector related). Concerning the TRIGA reactor available at LENA, simulations and preliminary tests, aiming at the neutron beam characterization, showed promising results, notwithstanding the limited reactor power (250 KW) and the limited daily working duty-cycle (6 hours, four days a week) [14].

The beam-port B of the TRIGA reactor (radial port, facing on the moderator) has the best potential for thermal NI applications, as it exhibits the highest ratio of thermal neutron with respect to the total neutron flux. The flight tube contains 70 mm bismuth and 100 mm sapphire filters to lower gamma and epithermal flux. The Monte Carlo N-Particle (MCNP) radiation transport code [15] was used to simulate the flux at the shutter beam position which turned out to be 1.6×10^7 $cm^{-2}s^{-1}$ for the thermal component, 3.5×10^5 $cm^{-2}s^{-1}$ for the epithermal component, and 2.1×10^5 $cm^{-2}s^{-1}$ for the fast component. The evaluated gamma flux is $\sim 10^6$ $cm^{-2}s^{-1}MeV^{-1}$ in the range 1-5 MeV [14]. These results make this beam port potentially suitable for thermal NI. The neutron shutter is located at the external wall of the TRIGA reactor monolith, approximately at 4.12 m from the reactor core.

Instrumental setup

An experimental hutch was already built around the B port shutter with constraints related to the available space and the multiple use of such port for other experimental activities, as shown in the aerial view of figure 1A. The size and shape are: 2.5 m length, 0.6 m minimum width, 2.1 m height, entrance area with double corner labyrinth. These imposed constraints imply strict limitations to the mechanical design of the imaging experimental station.

Beam collimation for imaging purposes is based on the use of removable and interchangeable cartridges (830 mm away from the shutter external wall) made of borated ceramic tiles [16] with variable pin-hole diameter (5, 10, 20, 30, 40, and 50 mm size).

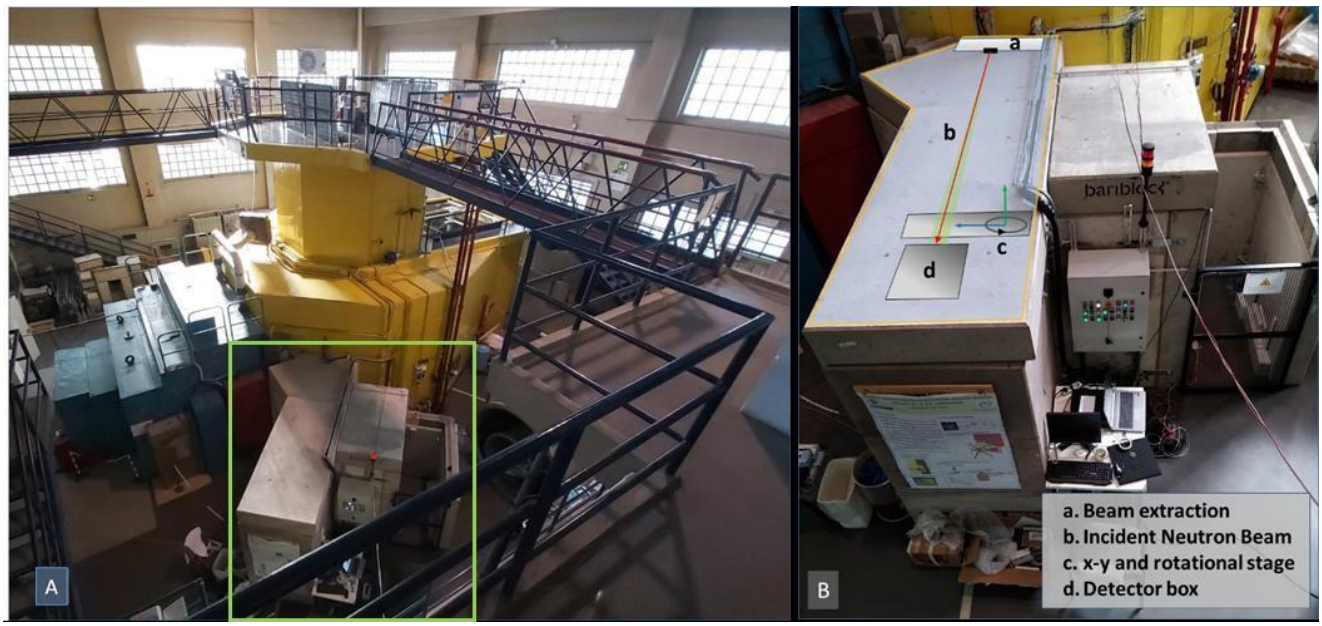

Fig. 1 A: panoramic view of the TRIGA reactor at LENA laboratory, including the port B experimental hutch (highlighted in green) where the NICHE set-up is host. **B:** superimposed schematic diagram of the NICHE set-up main components and aerial view of the experimental hutch.

The sample position area allows for its horizontal and vertical translation (orthogonal to the beam) and rotation around a vertical axis. Two linear stages using precision stepper-motors allow the horizontal and vertical translation, while rotation is made by a PI M-060 stage. All translation and rotation stages are remotely controlled.

The imaging camera box is composed by a 300 µm-thick ^{6}LiF/ZnS(Ag) scintillator screen 200x200 mm wide, followed by a 45° mirror, a 35 mm focusing lens and a ZWO ASI 2600 MM pro CMOS camera (16 bit). Lens focusing and camera operation are both remotely controlled. Pixel size corresponds to 30x30 µm^2 on the scintillator in the current configuration, allowing for a field of view (FOV) of 180x120 mm^2. The 45° mirror is used to limit the radiation damage induced by the neutron beam to the CMOS camera. A light-tight camera box houses the whole system. Remote control of the sample positioning, the lens focusing and the camera system is operated via ARDUINO Mega, using an in-house developed software in the LabView 2018 SP1 environment. The code is designed to perform multiple command sequence, allowing the execution of sequential radiographies in different areas of the sample and the acquisition of tomographic projections, if necessary. A scheme of the neutron imaging set-up components is shown in figure 1B.

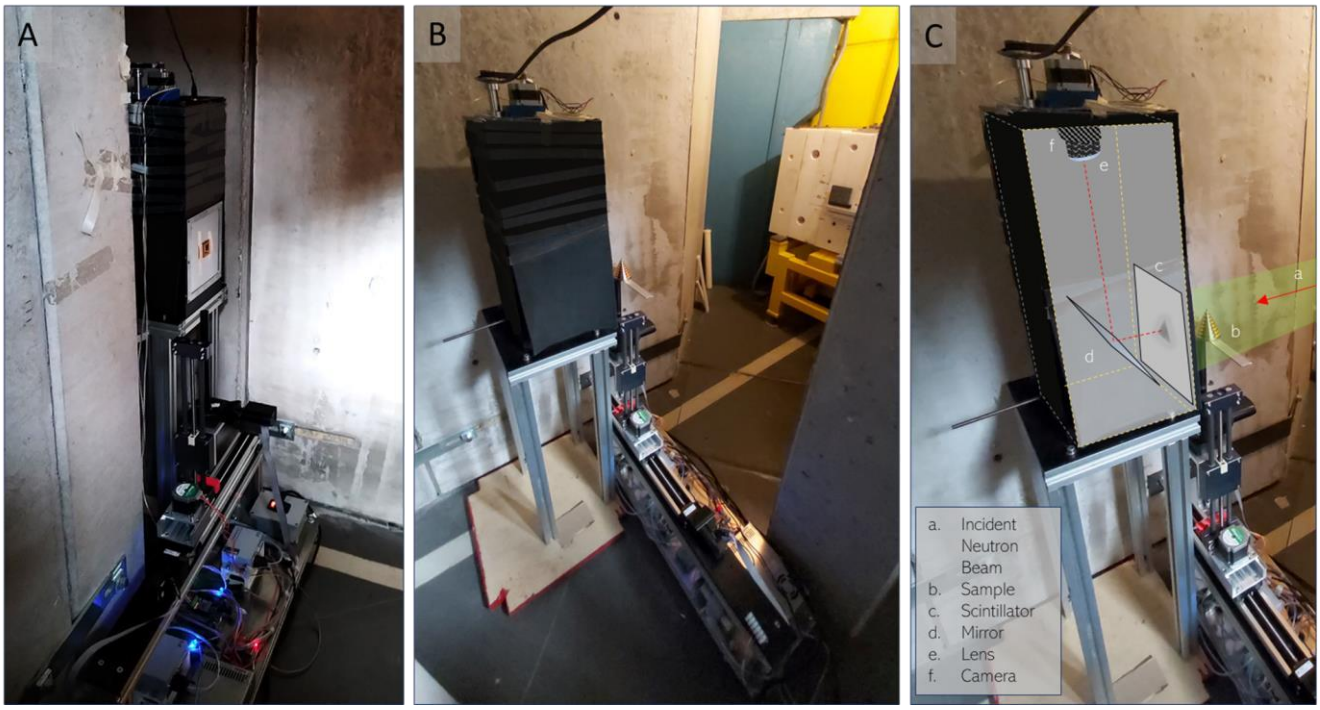

Fig. 2 A-B: Pictures showing sample translation and rotation stages, and the detector camera box. **C**: Picture and sketch of the optical components within the camera box.

A few pictures of the inner area of the NICHE experimental hutch are shown in figure 2A and 2B. The details of the camera box components are shown in figure 2C.

Characteristics and performances

In order to maximize the flexibility of the NICHE imaging station, we selected two extreme working positions exhibiting, respectively, the highest flux and the highest spatial resolution. These two configurations correspond to the minimum (position A table 1) and maximum (position B table 1) possible distance between the sample and the pin-hole. The L/D ratio (L is the distance between the pin-hole and the sample; D is the diameter of the pin-hole) is the parameter commonly used to define the resolution power of an imaging system. We decided to provide specifications for the 10 mm-diameter pin-hole because it maintains a reasonably short exposure time together with an acceptable resolution, while the improvement in flux of larger pin-hole configurations does not compensate for the reduction in resolution.

The resolution of the radiographs has been estimated in the different working conditions by using several spatial resolution reference samples, such as the “bar pattern” and “Siemens star” produced and distributed by the Paul Scherrer Institut (PSI) [17]. The best resolution was measured by sticking a Gd reference sample, based on bar pattern grid, directly on the scintillator.

A: pin-hole to sample distance 140 cm	**B: pin-hole to sample distance 190 cm**
L/D □ 140	L/D □ 190
Field of view: D = 65 mm, S = 45 mm	Field of view: D = 95 mm, S = 65 mm
Best spatial resolution: 150 µm	Best spatial resolution: 125 µm
Radiography Acquisition time: 300 s	Radiography Acquisition time: 600 s

Table 1 Basic imaging parameters in two different experimental configuration maximizing flux (A) or resolution (B). The best resolution was measured by sticking a Gd reference sample, based on bar

pattern grid, directly on the scintillator; D = diameter of the full brightness area of the neutron beam, and S = side of the inscribed square.

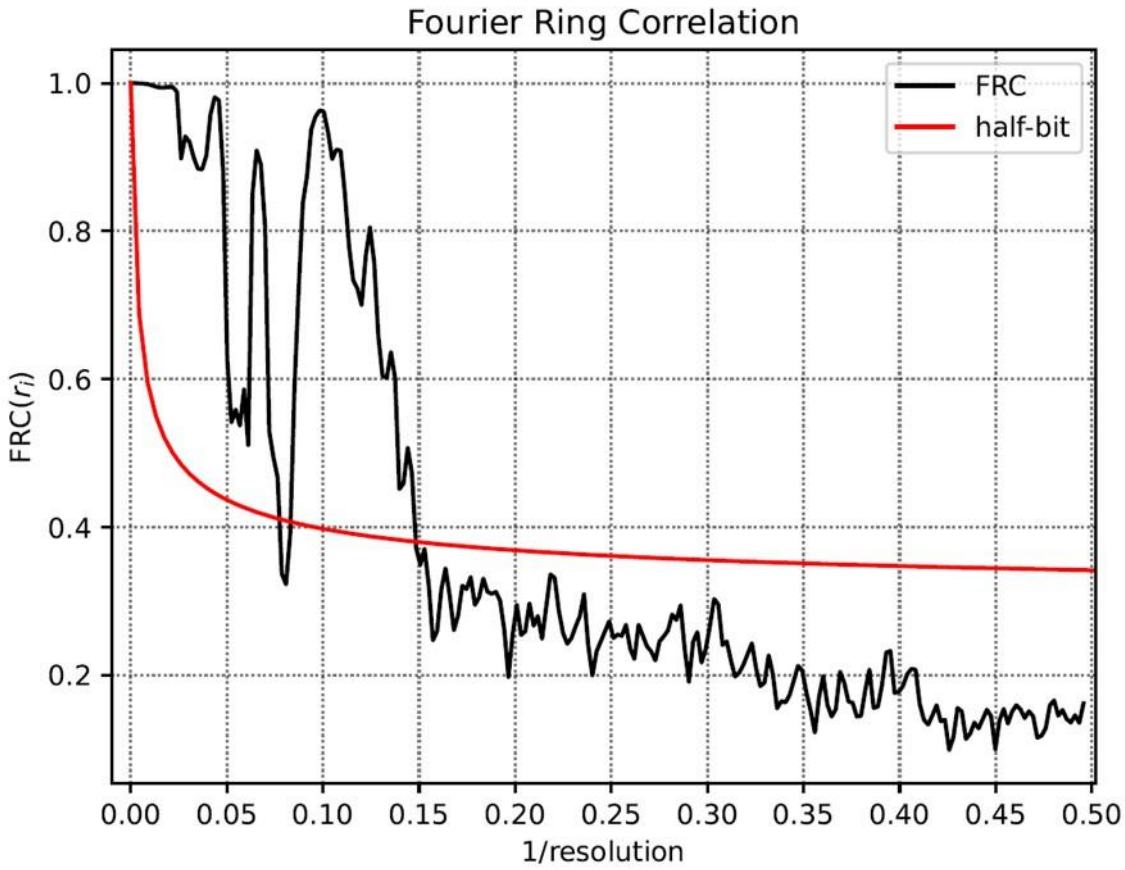

Fig. 3. FRC analysis of Siemens star sample at 50 mm distance from scintillator (L/D=140) providing a resolution of 30 / 0.15 µm.

An accurate evaluation of the resolution can be achieved by applying the Fourier Ring Correlation (FRC) method to a set of two twin images taken on the same sample in the same experimental configuration and performing a frequency analysis [18]. An example of FRC application is shown in figure 3, where a set of images of a Siemens star [17] was acquired at NICHE at 50 mm sample-to-scintillator distance (L/D=140), a typical working distance for a complex geometry sample, and exhibiting an intersection point between data and half bit function threshold [19] at 0.15 unit / resolution. The resolution value is obtained by dividing the pixel size by such a parameter, thus providing an effective resolution of 200 µm for samples in the typical measuring position (50 mm distance from scintillator).

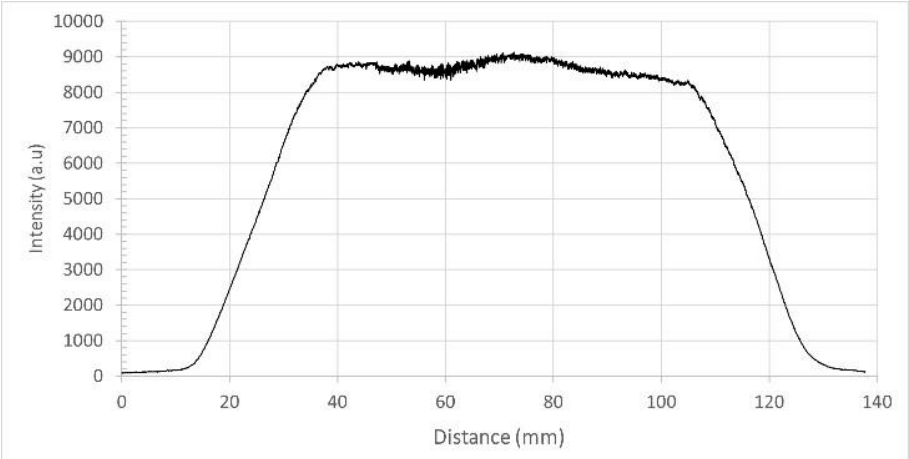

Fig. 4 Beam intensity profile at its horizontal diameter, showing good uniformity in the central area. It also allows for the measurement of the full brightness field of view, which results to be about 9 cm FWHM at 190 cm from the pin-hole.

In figure 4, the beam intensity profile is reported, showing good uniformity in the central area. The analysis of sample image raw data was performed by using the free software package ImageJ [20]. As a first step, we apply on every image a "spot filter" to remove the pixels that "shoot" anomalously due to gamma radiation; after that, it is always necessary to subtract the "dark" image from the raw intensity data: in this way we can take into account the CMOS dark current. The background-subtracted sample image is then normalised dividing it by applying open beam image normalisation to erase effects related to variations in incident intensity.

In the following part of the paper, we report some selected examples of neutron radiographs acquired with NICHE, showing the potential of the facility in terms of field of view, contrast, and spatial resolution for a large variety of flat and 3D samples, made up of different combinations of materials. In this way, it is possible to evaluate the capability of morphological analysis in composite objects, and the ability to differentiate among various constituents.

Figure 5 shows two open beam corrected (normalised) radiographs taken with L/D=190 and the samples positioned at 40 mm from the scintillator screen, using 300 s integration time.

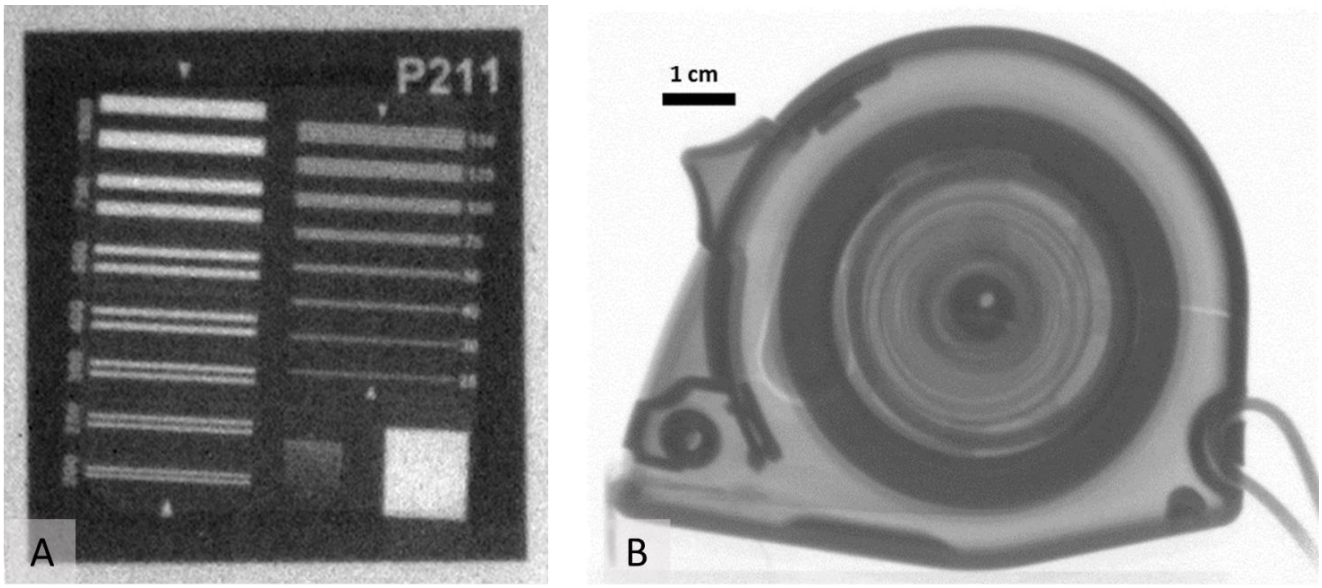

Fig. 5 Neutron radiographs collected at L/D=190, integration time 300 s, sample-to-scintillator distance 40 mm. **A:** the PSI bar pattern (25 mm side length) devoted to spatial resolution estimation; **B:** rolled metal tape with plastic case.

Figure 5A shows the PSI bar pattern radiography, that allows to estimate the spatial resolution of the system by mapping which of the tilted lines are visible and well-resolved according to their size and inter-spacing, 150 µm in this case. The radiograph of a rolled tape metre (fig. 5B) shows the assembled structure containing a metal tape encased within a plastic frame. Different grey tones reveal the arrangement of the rolled tape and of the mechanical joints of the case.

It is possible to perform neutron radiographs of samples larger than the neutron beam spot size by using the horizontal and vertical translations stages. We can move the sample to take partial radiographs in different positions and later recombine them. However, present spatial constraints in the experimental hutch do not allow full coverage of objects larger than 25 cm.
In order to test the stitching procedure, we choose to cover the whole area occupied by a moka pot (inspired by A. Kaestner [21]) by taking four radiographs arranged in a 2x2 grid. The composite normalised image, obtained by using pairwise stitching ImageJ tool [22] is shown in figure 6, where it is evident that no stitching artefacts are visible. In the image it is possible to observe several interesting

features, such as the different attenuation power of coffee powder, the aluminium case, the water reservoir and also the water droplets dispersed in the upper chamber of the coffee machine and on the lid. Red-squared insets highlight selected areas in which further details are pointed out by adjusting brightness and contrast.

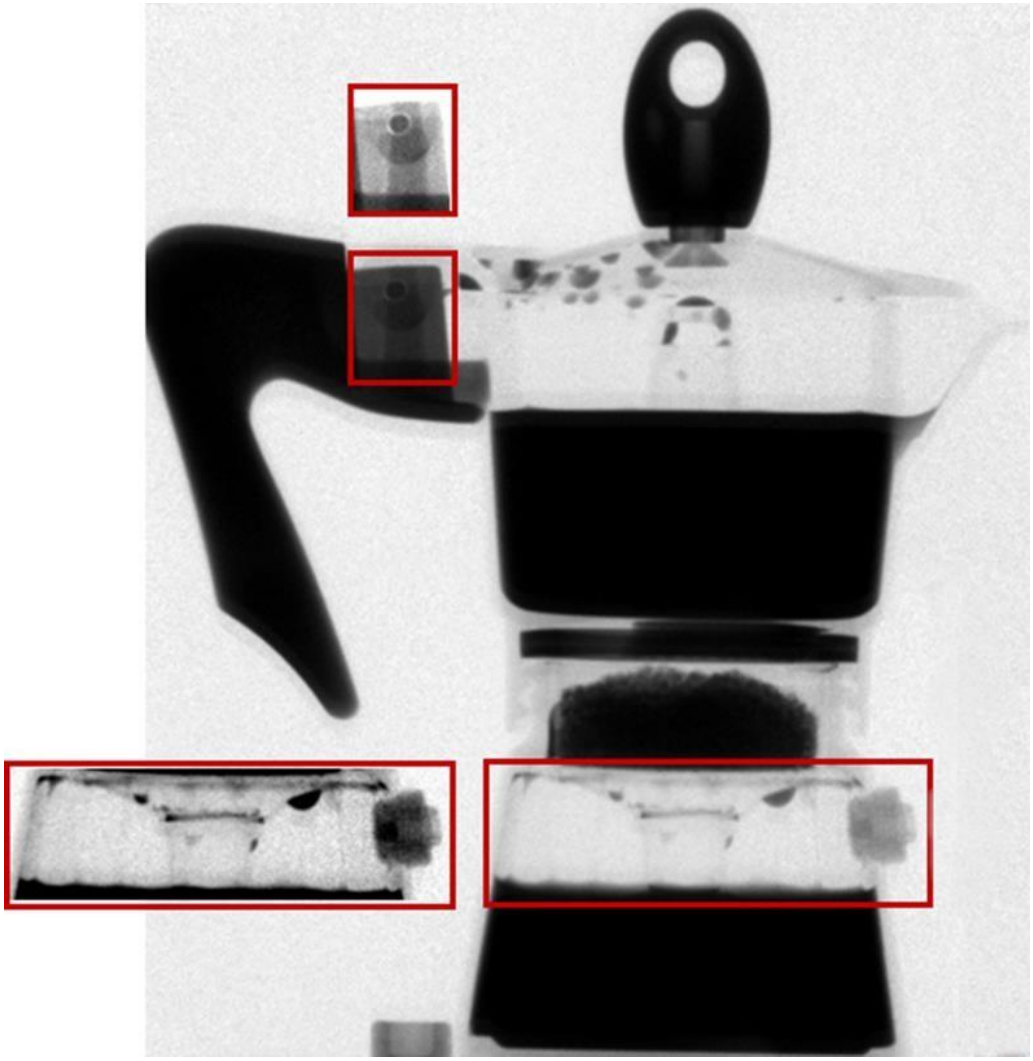

Fig. 6 Composite radiograph of a moka pot, obtained as a mosaic of 2x2 neutron images, stitched together. The insets show inner structure and connecting parts of the machine case.

Neutron tomography was performed by exploiting the sample rotating stage. Because of the large number of projection images (minimum 300 according to pixel size and imaging station spatial resolution) and the minimum time needed for each of them in order to have an acceptable signal to noise ratio (120 s), a tomography requires at least two operational days at LENA to be completed.

As an example, we show, in figure 7, the tomographic reconstruction of a plastic figure. Data were processed using Octopus [23] for reconstruction and different ImageJ spatial linear and radial filters [20] to preliminary process the projections. The 3D rendering was performed by using 3D Slicer 4.11 [24].

It is interesting to note the capability of the system to highlight the plastic parts with very good spatial definition, notwithstanding the high incoherent scattering power of such hydrogen-rich material.

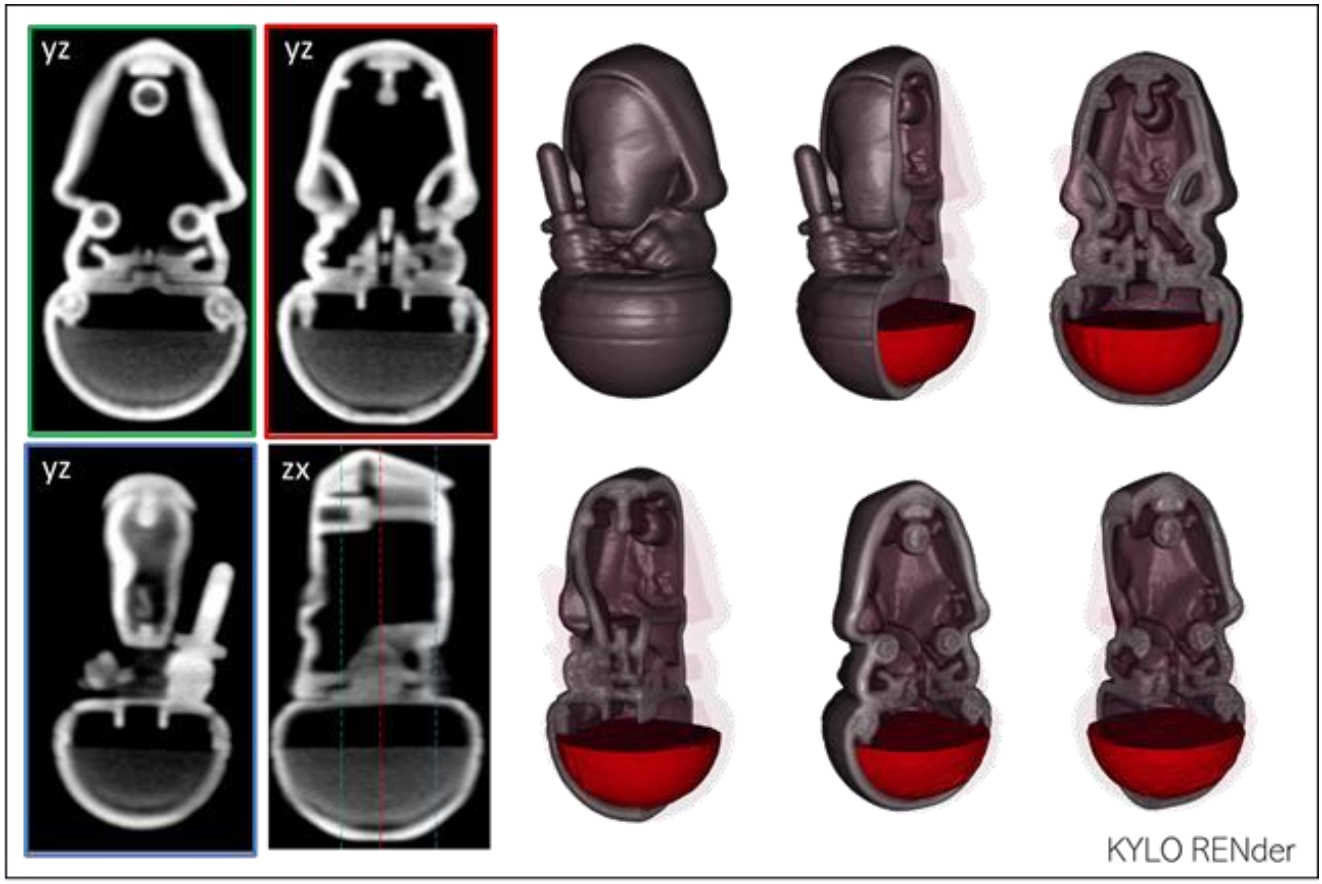

Fig. 7 Example of results of neutron tomography on a plastic model (approx. 3.5 cm height). 3D rendering and sectioning show the inner structure.

Conclusions

The commissioning of the new Neutron Imaging facility is completed and the NICHE station is currently fully operative at the TRIGA reactor of the LENA laboratory.
NICHE is integrating the diagnostic instrumentation already owned by the INFN-CHNet and widening the range of available technologies of the network.
It allows the acquisition of single radiographs with good spatial resolution (up to 125-150 □m) and a maximum field of view of about 9 cm (diameter).
The sample positioning remote system allows carrying out measurements even on objects larger than the field of view, by making multiple radiographs and stitching them without introducing artefacts or discontinuities. The system also allows the acquisition of tomographies, still with effective spatial resolution (better than 250 □m) and contrast suitable for material science analysis.
The NICHE neutron imaging station will allow to perform case studies of interest in the field of CH, providing morphological and microstructural information not obtainable with the more conventional X-ray imaging.

Statements

The authors have no relevant financial or non-financial interests to disclose.

Acknowledgment

This work has been funded by INFN, via the CHNet-NICHE CSN 5 experiment, and by INFN-CHNet network. The support of A. Catelani, N. Pasqualetti and M. Leporatti of the Mechanical Workshop of the Department of Physics and Astronomy of the University of Firenze is acknowledged with gratitude. The authors would like to thank the LENA personnel, who have provided great support to the experimental work well beyond their possibilities.

Author contributions

All authors have given their contribution to the experimental work and the production of the paper, each one in her/his proper field of expertise.

Data Availability Statement

The datasets generated and/or analysed during the current study are available from the corresponding author on reasonable request.

References

[1] Giuntini, L., Castelli, L., Massi, M., Fedi, M., Czelusniak, C., Gelli, N., Liccioli, L., (...), Taccetti, F. (2021)
Detectors and cultural heritage: The INFN-CHNet experience, Applied Sciences, 11, 3462, https://www.mdpi.com/2076-3417/11/8/3462/pdf

[2] Taccetti, F., Castelli, L., Czelusniak, C., Gelli, N., Mazzinghi, A., Palla, L., Ruberto, C., (...), Giuntini, L., (2019) A multipurpose X-ray fluorescence scanner developed for in situ analysis, Rendiconti Lincei, 30 (2), pp. 307-322, http://www.springerlink.com/content/120941/ , https://doi.org/10.1007/s12210-018-0756-x

[3] Lehmann, Eberhard H., Eckhard DESCHLER-ERB, and A. Ford. "NEUTRON TOMOGRAPHY AS A VALUABLE TOOL
FOR THE NON-DESTRUCTIVE ANALYSIS OF HISTORICAL BRONZE SCULPTURES." Archaeometry 52.2 (2010): 272285, https://doi.org/10.1111/j.1475-4754.2009.00480.x

[4] Lehmann, Eberhard H., Stefan Hartmann, and Markus O. Speidel. "Investigation of the content of ancient Tibetan metallic Buddha statues by means of neutron imaging methods." Archaeometry 52.3 (2010): 416-428, https://doi.org/10.1111/j.1475-4754.2009.00488.x

[5] Fedrigo, Anna, et al. "Neutron imaging study of 'pattern-welded'swords from the Viking Age." *Archaeological and Anthropological Sciences* 10.6 (2018): 1249-1263.

[6] Grazzi, Francesco, et al. "Characterization of two Japanese ancient swords through neutron imaging." 波紋 25.3 (2015): 206-213.

[7] Kino, K., et al. "Analysis of crystallographic structure of a Japanese sword by the pulsed neutron transmission method." Physics Procedia 43 (2013): 360-364, https://doi.org/10.1016/j.phpro.2013.03.043

[8] Depalmas, A., et al. "Neutron-based techniques for archaeometry: characterization of a Sardinian boat model." Archaeological and Anthropological Sciences 13.6 (2021): 1-9, https://doi.org/10.1007/s12520-02101345-w

[9] Salvemini, Filomena, et al. "Non-invasive characterization of ancient Indonesian Kris through neutron methods." *The European Physical Journal Plus* 135.5 (2020): 1-25.

[10] Salvemini, F., Grazzi, F., Fedrigo, A. et al. "Revealing the secrets of composite helmets of ancient Japanese tradition." Eur. Phys. J. Plus 128, 87 (2013). https://doi.org/10.1140/epjp/i2013-13087-y

[11] Salvemini, F. et al. "On the use of neutron imaging methods to identify microstructural features in ancient
Indian swords and armour." Microchemical Journal 159 (2020): 105397, https://doi.org/10.1016/j.microc.2020.105397

[12] Prata, M., et al, "Italian neutron sources" Eur. Phys. J. Plus 129: 255 (2014), https://doi.org/10.1140/epjp/i2014-14255-3

[13] Anderson I.S. et al., Research opportunities with compact accelerator-driven neutron sources, Physics Reports, Volume 654, 2016, Pages 1-58, https://doi.org/10.1016/j.physrep.2016.07.007

[14] Salvini, A., et al. "Design, implementation and future utilization of the PGNAA facility at the University of Pavia–Lena Laboratory." *Research Reactors: Addressing Challenges and Opportunities to Ensure Effectiveness and Sustainability. Summary of an International Conference. Supplementary Files*. 2020.

[15] Werner, Christopher John, et al. *MCNP version 6.2 release notes*. No. LA-UR-18-20808. Los Alamos National Lab.(LANL), Los Alamos, NM (United States), 2018.

[16] Celli, M., Grazzi, F., & Zoppi, M. (2006). A new ceramic material for shielding pulsed neutron scattering instruments. *Nuclear Instruments and Methods in Physics Research Section A:*

Accelerators, Spectrometers, Detectors and Associated Equipment, *565*(2), 861-863. DOI: 10.1016/j.nima.2006.05.234

[17] Trtik, Pavel, et al. "Improving the spatial resolution of neutron imaging at paul scherrer institut–the neutron microscope project." *Physics Procedia* 69 (2015): 169-176.

[18] Van Heel, Marin. "Similarity measures between images." *Ultramicroscopy* 21.1 (1987): 95-100.

[19] Van Heel, Marin, and Michael Schatz. "Fourier shell correlation threshold criteria." *Journal of structural biology* 151.3 (2005): 250-262.

[20] Abràmoff, Michael D., Paulo J. Magalhães, and Sunanda J. Ram. "Image processing with ImageJ." *Biophotonics international* 11.7 (2004): 36-42.

[21] https://www.psi.ch/

[22] Preibisch, S., Saalfeld, S., & Tomancak, P. (2009). Globally optimal stitching of tiled 3D microscopic image acquisitions. *Bioinformatics*, *25*(11), 1463-1465.

[23] Dierick, Manuel, Bert Masschaele, and Luc Van Hoorebeke. "Octopus, a fast and user-friendly tomographic reconstruction package developed in LabView®." *Measurement Science and Technology* 15.7 (2004): 1366. [24] Uday, Patil Abhishek, Naiknimbalkar Digvijay, and J. B. Jeeva. "Pre-operative brain tumor segmentation using SLICER-3D." *2014 international Conference on green computing communication and electrical engineering (ICGCCEE)*. IEEE, 2014